Evaluation of Modeling Water-Vapor-Weighted Mean Tropospheric Temperature for GNSS-Integrated Water Vapor Estimates in Brazil

LUIZ F. SAPUCCI

Centro de Previsão de Tempo e Estudos Climáticos, Instituto Nacional de Pesquisas Espaciais, Cachoeira Paulista, São Paulo, Brazil

(Manuscript received 4 February 2013, in final form 29 October 2013)

ABSTRACT

Meteorological application of Global Navigation Satellite System (GNSS) data over Brazil has increased significantly in recent years, motivated by the significant amount of investment from research agencies. Several projects have, among their principal objectives, the monitoring of humidity over Brazilian territory. These research projects require integrated water vapor (IWV) values with maximum quality, and, accordingly, appropriate data from the installed meteorological stations, together with the GNSS antennas, have been used. The model that is applied to estimate the water-vapor-weighted mean tropospheric temperature (Tm) is a source of uncertainty in the estimate of IWV values using the ground-based GNSS receivers in Brazil. Two global models and one algorithm for Tm, developed through the use of radiosondes, numerical weather prediction products, and 40-yr ECMWF Re-Analysis (ERA-40), as well as two regional models, were evaluated using a dataset of ~78 000 radiosonde profiles collected at 22 stations in Brazil during a 12-yr period (1999–2010). The regional models (denoted the Brazilian and regional models) were developed with the use of multivariate statistical analysis using ~90 000 radiosonde profiles launched at 12 stations over a 32-yr period (1961–93). The main conclusion is that the Brazilian model and two global models exhibit similar performance if the complete dataset and the entire period are taken into consideration. However, for seasonal and local variations of the Tm values, the Brazilian model was better than the other two models for most stations. The Tm values from ERA-40 present no bias, but their scatter is larger than that in the other models.

1. Introduction

Using Global Navigation Satellite System (GNSS) data collected by ground-based receivers to determine the amount of integrated water vapor (IWV) has provided good quality data with high temporal resolution to the research community (Bevis et al. 1992; Rocken et al. 1997; Emardson and Derks 2000; Deblonde et al. 2005). The application of this technique using GNSS receiver networks produces measurements of the total-column water vapor content of the troposphere over the entire globe. The IWV values from GNSS data have been used with success to evaluate the quality of data from other instruments, such as photometers (Ingold et al. 2000; Sapucci et al. 2007), radiosondes (Deblonde et al. 2005), and radiometers (Liou et al. 2001; Van Baelen et al. 2005 and others), or to validate numerical weather prediction (NWP) models (Guerova et al. 2003) or methods for obtaining GNSS IWV estimates in real time, such as that of Dick et al. (2001).

There are several developing research projects that aim to monitor the humidity over Brazilian territory using a network of ground-based GNSS receivers. This network has been made denser over recent years. Two projects for increasing the network density should be mentioned: the GNSS-SP (São Paulo State GNSS network) project, involving local networks in the São Paulo State (Monico et al. 2009), and the Integrated System of GNSS Positioning for Geodynamic Studies (SIPEC) project, aimed at areas of difficult access in Brazil, such as forests in the Amazon region and islands along the Brazilian oceanic coast. The CHUVA project (information online at http://chuvaproject.cptec.inpe.br/portal/noticia.ultimas.logic?i=en) has performed several experiments in different parts of Brazil. The main objective is to understand the physical processes that occur inside clouds during storms. The GNSS receiver network

Corresponding author address: Luiz F. Sapucci, Instituto Nacional de Pesquisas Espaciais, CPTEC, Rodovia Presidente Dutra, km 40, CEP 12630, Cachoeira Paulista, São Paulo, Brazil.
E-mail: luiz.sapucci@cptec.inpe.br

DOI: 10.1175/JAMC-D-13-048.1

has been used in these experiments to provide IWV series with good quality and high temporal resolution, which are used to monitor the horizontal variations in the integrated water vapor before, during, and after heavy precipitation events. Another project in development applies a dense GNSS meteorological network to track water vapor advection and to identify convective events and water vapor convergence time scales in the Amazon region (Adams et al. 2011). All of these research projects require IWV values with maximum quality, suitable for possible use in any of these meteorological applications, and, thus, considerable effort has been made to minimize the error in the IWV retrieval technique using GNSS data. The main sources of uncertainty in this technique are 1) GNSS data processing, 2) appropriate meteorological observations at the GNSS antenna locations, and 3) suitable modeling of the water-vapor-weighted mean tropospheric temperature (Tm) (Emardson and Derks 2000). The latest-generation scientific software, such as the GNSS-Inferred Positioning System and Orbit Analysis Simulation Software package (GIPSY) and the Orbit Analysis Simulation Software (OASIS), collectively known as GOA-II (Gregorius 1996), and GPS Analysis at the Massachusetts Institute of Technology (GAMIT; Herring et al. 2012), has been used in the processing of the GNSS data collected in the mentioned experiments, together with observations from specially installed meteorological stations linked to the GNSS receivers. To minimize the remaining sources of uncertainty, this paper studies the impact of existing Tm modeling on the quality of the IWV values obtained from ground-based GNSS receivers over Brazilian territory and identifies the most suitable models. This possible improvement in Tm modeling can have positive consequences for NWP or climate studies in this region, where long-term time series of IWV with better quality data will be available.

The application of GNSS to the quantification of IWV began with the studies performed to try to minimize the influence of the variation in the index of refraction along the electromagnetic signal propagation path through the atmosphere. A relationship between the amount of atmospheric water vapor and the delay in the electromagnetic signal propagation was demonstrated (Askne and Nordius 1987). This early work led to a method for estimating the IWV values from the zenith tropospheric delay (Bevis et al. 1992). The quantity Tm (Davis et al. 1985) is an approximation of the relationship between the humidity and temperature profiles; consequently, the accuracy of the GNSS estimates of the IWV is directly related to the accuracy of Tm (Bevis et al. 1994). Because Tm depends on the vertical profiles of temperature and humidity, it varies from region to region as well as seasonally, and, therefore, a long-term radiosonde dataset is necessary to assess its real variability. The Tm values can be estimated from site-specific historical data using means or statistical relationships from the measurements at the surface (Ross and Rosenfeld 1997). Using 8700 radiosonde profiles collected at 13 U.S. stations over a 2-yr period, Bevis et al. (1992) developed the first Tm model, which estimates Tm from the observed surface temperature by applying linear regression.

Similar Tm models to that of Bevis et al. and other more sophisticated models were developed for several regions, and other models were developed for the global domain. Three versions of the Tm model were developed for the European region using over 120 000 radiosonde profiles from 38 stations (Emardson and Derks 2000): the first is based on a simplified physical model, the second used polynomial regression, and the third is based only on the seasonal variation in Tm. Mendes et al. (2000) presented a global model based on a linear regression using ~32 500 radiosonde profiles from 50 dispersed stations over the entire globe for the year 1992. A comparison of this global model with other European models suggested by Emardson and Derks (2000) indicated that results of similar precision are obtained by both types of models in the European region (Mendes et al. 2000). In addition to developing models from radiosonde datasets, atmospheric profiles from a NWP model have also been used in Tm modeling. Schueler et al. (2001) used global fields from numerical models of the National Centers for Environmental Prediction (NCEP) and proposed three global models: the harmonic model, the linear surface temperature model, and the mixed harmonic-temperature model. The results of the evaluation demonstrated that IWV values with a satisfactory degree of accuracy (range of 0.2–0.3 $\mathrm{kg\,m^{-2}}$) can be obtained from GNSS data anywhere in the world by the application of the mixed harmonic-temperature model (Schueler et al. 2001). For example, this mixed model has been used in the analysis of GNSS IWV data in India (Jade et al. 2005). Reanalysis data have also been used in Tm modeling. The Tm values have been estimated using temperature and humidity profile data from both the 40-yr European Centre for Medium-Range Weather Forecasts (ECMWF) Re-Analysis (ERA-40) and the NCEP–National Center for Atmospheric Research (NCAR) reanalysis (Wang et al. 2005). Verification against a global radiosonde dataset demonstrated that both reanalyses produced reasonable Tm estimates; however, the ERA-40 dataset was concluded to be a better choice for global Tm estimation because of its superior performance and its higher spatial resolution (Wang et al. 2005). The Tm modeling using ERA-40 reanalysis has been used in work involving the evaluation of the IWV fields from the NCEP–NCAR

reanalysis using one decade of postprocessed Global Positioning System (GPS) data (Vey et al. 2010).

The present paper compares the quality of the Tm values generated from the existing global models and from two new regional models over Brazil. These regional models were developed using multivariate statistical analysis applied over ~90 000 radiosonde profiles launched at 12 Brazilian stations during the period from February 1961 to May 1993. An independent set of ~78 000 radiosonde profiles collected in Brazil at 22 stations during the period from 1999 to 2010 (12 yr) was used as an independent verification dataset. The global and regional models evaluated are described, and information about the temporal and spatial distributions of radiosondes used in the evaluation of available models over Brazil is presented in section 2. In section 3, the methodology used to evaluate the models and the results obtained are presented. A summary of the work and the conclusions are presented in section 4. Appendix A presents the role of the water-vapor-weighted mean tropospheric temperature in the IWV quantification from GNSS data, and appendix B the dataset and the methodology used in the regional modeling of Tm over Brazil are described, and two models are proposed.

2. Models evaluated and datasets employed

The value of Tm can be extracted from the values for the air temperature (T) and the partial pressure of the water vapor (e) at each level (h) of the atmospheric profiles as follows:

$$\mathrm{Tm} = \frac{\int \frac{e}{T}\partial h}{\int \frac{e}{T^2}\partial h}, \tag{1}$$

which is the solution presented by Davis et al. (1985) to solve the dependence of upper-air profile information upon the IWV values obtained from the GNSS data. The role played by the Tm values in this process and their derivation from the mean value theorem for integration are demonstrated in appendix A.

The evaluated models are the linear regression suggested by Mendes et al. (2000), the three versions developed by Schueler et al. (2001), the values based on ERA-40, and two regional models (regional and Brazilian) developed using ~90 000 radiosonde profiles launched over Brazil territory, which are hereafter denoted MENDE, SCHU1, SCHU2, SCHU3, ERA-40, REGIO, and BRAZI, respectively. More details about each model are presented below.

a. Global models evaluated

The global model presented by Mendes et al. (2000) is based on a linear regression between the surface temperature (Ts) and the Tm values, expressed by the following formula:

$$\mathrm{Tm} = 0.789\mathrm{Ts} + 50.4. \tag{2}$$

The parameters were determined using ~32 500 radiosonde profiles from 50 stations, covering a latitude range of 62°S–83°N, all launched in 1992. Seven stations used in this model are located in Brazil.

Schueler et al. (2001) used global NWP fields from NCEP to develop three global models. The first is a harmonic model based on an average mean atmospheric temperature ($\overline{\mathrm{Tm}}$) and on the amplitude of the annual cycle of mean temperature ($\widetilde{\mathrm{Tm}}$), which is specific for each station. The values provided by Brazilian stations were used here; however, the tabulated value of $\widetilde{\mathrm{Tm}}$ is zero at Brazilian stations (Schueler et al. 2001), and, consequently, this model yields a constant value (Tm = 275.85). The second model is based on a linear regression between the surface temperature and the Tm values. This second model is given by the expression

$$\mathrm{Tm} = 0.647\mathrm{Ts} + 86.9. \tag{3}$$

The third model is a combination of the previous approaches, which yields the mixed harmonic and surface temperature model. The Tm values at the requested day of the year (DoY) can be expressed by the equation

$$\mathrm{Tm} = \overline{\mathrm{Tm}} + \widetilde{\mathrm{Tm}}\cos\left[2\pi\frac{\mathrm{DoY} - \mathrm{DoYw}}{365.25\,(\mathrm{days})}\right] + \mathrm{qT}\,\mathrm{Ts}, \tag{4}$$

where DoYw is the day of "maximum winter" (day 28 for the Northern Hemisphere and day 211 for the Southern Hemisphere) and qT is an amplifier-weighting term for the surface temperature (Schueler et al. 2001).

The methodology used to determine Tm employing the temperature and humidity profiles from the ERA-40 reanalysis reported by Wang et al. (2005) is also evaluated here. The comparison with radiosonde profiles was conducted by applying vertical extrapolation and linear horizontal interpolation of the reanalysis profiles in Eq. (1), and the Tm values were determined at the radiosonde locations (Wang et al. 2005). The average temperature lapse rates for the first three levels and the average humidity for the first two levels were used in the vertical extrapolation. The ERA-40 reanalysis was used instead of the NCEP–NCAR reanalysis because Wang et al. (2005) demonstrated that the former exhibits better performance and higher resolution than the latter.

TABLE 1. Location, ID number, and number of radiosondes used in the modeling (in appendix B) and in the evaluation of the Tm models over Brazilian territory.

City, federal unit	Station ID	WMO No.	Lat	Lon	Elev (m)	Quantity of radiosondes	
						Modeling	Evaluation
Belém, Pará	BELE	82193	1°22′S	48°28′W	16.0	5952	5356
Manaus, Amazonas	MANA	82332	3°08′S	59°59′W	85.0	7577	6043
Fortaleza, Ceará	FORT	82397	3°46′S	38°36′W	3.0	—	2135
Fernando de Noronha, Pernambuco	FEDN	82400	3°51′S	32°25′W	56.0	2732	1308
Natal, Rio Grande do Norte	NATA	82599	5°54′S	35°14′W	52.0	5426	3377
Porto Velho, Rondônia	PORV	82824	8°46′S	63°55′W	85.0	—	2241
Recife, Pernambuco	RECF	82900	8°03′S	34°55′W	7.0	—	2221
Alta Floresta, Mato Grosso	ALFL	82965	9°52′S	56°06′W	288.0	771	—
Vilhena, Rondônia	VLHE	83208	12°41′S	60°05′W	615.0	3036	3292
Salvador, Bahia	SALV	83229	13°00′S	38°30′W	51.0	—	1781
Bom Jesus da Lapa, Bahia	BJDL	83288	13°15′S	43°24′W	440.0	—	1807
Cuiabá, Mato Grosso	CUAB	83362	15°39′S	56°06′W	182	—	4640
Brasília, Distrito Federal	BRAS	83378	15°52′S	47°55′W	1061.0	10 780	4455
Caravelas, Bahia	CARA	83498	17°44′S	39°15′W	4.0	—	1414
Corumbá, Mato Grosso do Sul	CORU	83554	19°00′S	57°40′W	142.0	—	2374
Belo Horizonte, Minas Gerais	CONF	83566	19°37′S	43°58′W	827.0	—	3146
Campo Grande, Mato Grosso do Sul	CAGR	83612	20°28′S	54°40′W	560.0	5311	4048
Trindade, Rio de Janeiro	TRND	83650	20°30′S	29°19′W	5.0	—	2393
Rio de Janeiro, Rio de Janeiro	RDJA	83746	22°48′S	43°14′W	21.0	13 613	6178
São Paulo, São Paulo	SAPA	83779	23°30′S	46°38′W	792.0	10 351	—
Curitiba, Paraná	CURT	83840	25°31′S	49°10′W	908.0	10 835	5899
Florianópolis, Santa Catarina	FLOR	83899	27°40′S	48°32′W	5.0	—	3650
Uruguaiana, Rio Grande do Sul	URUG	83928	29°46′S	57°02′W	62.0	—	3820
Porto Alegre, Rio Grande do Sul	POAL	83971	29°59′S	51°10′W	47.0	13 230	6517
		Total				89 614	78 095

b. *Regional models evaluated*

Although the model proposed by Bevis et al. (1992) used only radiosonde data from across the United States, this model has been used in the application of GNSS data to the quantification of IWV over other regions (Ross and Rosenfeld 1997). However, Emardson (1998) demonstrated the importance of regionalization in Tm modeling. Liou et al. (2001) developed a model specific to Taiwan and demonstrated that the relationship between Tm and Ts is site dependent. Accordingly, new Brazilian regional models of Tm have been created using ~90 000 radiosonde profiles launched at 12 stations over a 32-yr period from February 1961 to May 1993. Multivariate statistical analysis was used to determine which surface variables are most effective for predicting the Tm values. The selected variables were pressure (Ps), temperature (Ts), relative humidity (RH), and the zonal (U) and meridional (V) wind components. Details about the dataset and the methodology used in this modeling are presented in appendix A, in which two models are proposed. The first model is denoted the Brazilian model and it can be expressed by the following formula:

$$\mathrm{Tm} = 0.558\mathrm{Ts} + 0.0105\mathrm{Ps} + 110.578. \quad (5)$$

The second model is denoted the regional model and it is given by the expression

$$\mathrm{Tm} = a\mathrm{Ts} + b\mathrm{Ps} + c\mathrm{RH} + d, \quad (6)$$

in which the values of the coefficients are listed in appendix B (see Table B3).

c. *Dataset used in the evaluation*

The radiosonde dataset used in the evaluation of the models is from the meteorological database at the Brazilian Center for Weather Prediction and Climate Studies (Centro de Previsão do Tempo e Estudos Climáticos, CPTEC). The sondes were launched at 22 stations during the period from January 1999 to August 2010. The total number of radiosondes used in the evaluation is 78 095. The cities from which these radiosondes were launched are listed in Table 1, along with the station identification number (ID) and coordinates and the number of radiosondes launched from each site. The stations located at São Paulo (SAPA station) and Alta Floresta (ALFL station) were not included in the evaluation because the data from these stations were not available in CPTEC's database. Figure 1 shows the spatial distribution of all the radiosonde stations used.

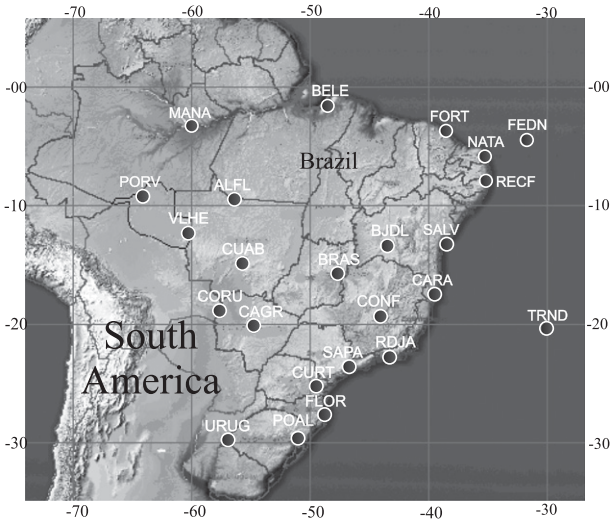

FIG. 1. Spatial distribution of radiosonde stations used in the modeling (in appendix B) and in the evaluation of the Tm model over Brazilian territory.

Figure 2 shows the temporal distribution of the data used in the evaluation. The period of data collection at each radiosonde station is also presented in Fig. 2, in which the frequency and regularity of the observations varies significantly from station to station.

3. Quality evaluation of the Tm model in Brazil

a. Evaluation methodology and analysis of the results

The radiosonde dataset was divided into two subsets because the ERA-40 reanalysis is available only up to 2002. The first set consists of the period from 1999 to 2002 (a total of 15 677 radiosondes), in which all models were evaluated. The second set consists of 78 095 radiosondes launched from 1999 to 2010, for which the ERA-40 reanalysis was not evaluated.

The results from the different models plotted against the Tm values from the radiosondes are shown in Fig. 3, which represents a scatter diagram from evaluated models for the two datasets into which the radiosondes were divided. The bias, standard deviation (SD), and root-mean-square error (RMSE) values using the Tm from the radiosondes as a reference are presented in Fig. 4. The bias values from the ERA-40 reanalysis and the BRAZI and REGIO models are less than 1 K. The SCHU3 and MENDE results exhibit a bias between -1 and -2, and for the SCHU1 and SCHU2 models, the bias exceeds -6 K. The SD values presented by the different models are very similar (SD values are approximately 2 K), except for ERA-40 and SCHU1, which produced SD values of 3.5 K. The ERA-40 scatter diagram can be assessed from Fig. 3b, which shows Tm values of lower precision than is found in the other models. The dataset used to evaluate ERA-40 was assimilated by this process; consequently, this reanalysis would be expected to present better results. A possible reason for this result could be the random error generated by the spatial resolution of ERA-40, which is not able to assess the temporal and spatial temperature variation closer to the radiosondes but is able to assess the temperature variation on a larger spatial scale. Another reason could be the dependence of the ERA-40 moisture on the model physics. Because the SCHU1 model is based on a constant value, the scatter of this model is dominated by the scatter of the Tm values from the radiosondes. The RMS error values presented by the REGIO and BRAZI models are similar and lower than those of the other models (RMSE of 2.2 K). The MENDE and SCHU3 models exhibit an RMS error of 2.9 K, the ERA-40 model exhibits an RMS error of 3.5 K, and the SCHU1 and SCHU2 models exhibit RMS errors greater than 7.0 K.

With regard to the variability of the Tm values from the radiosonde observations, used here as a reference, another way to present the results is to use a Taylor diagram (Taylor 2001). This diagram reveals the patterns of similarity among the different models and reference observations (radiosondes), which are determined in terms of the correlation coefficient, centered quadratic difference (RMSD), and standard deviation values from the radiosondes and the models. The same point on the diagram can represent these three statistical measurements. The radial distance from the origin is proportional to the standard deviation. The RMSD between the models and the radiosonde is proportional to their distance apart (in the same units as the standard deviation). The correlation between the two fields is given by the azimuthal position of the model evaluated. More details about the Taylor diagram are given in Taylor (2001). The first set of radiosondes was used to calculate the values needed to create the Taylor diagram for the different models and the reanalysis, and the resulting Taylor diagram is plotted in Fig. 5. The second dataset was not used in this analysis because the reanalysis is not evaluated in this case and the results from the other models are very similar to those shown in Fig. 5. The RMSD values from the SCHU2, REGIO, and BRAZI models are lower than those from the other models (RMSD of 0.63 K), and the ERA-40 exhibits the largest value (0.95 K). The correlation coefficient is 0.75 for all models except ERA-40, which has a correlation coefficient of 0.55. The standard deviation of SCHU3 is lower than that of the other models (SD of 0.4 K). Figure 6 shows the Tm error from the models and the reanalysis as a function of IWV, in which it is possible to determine

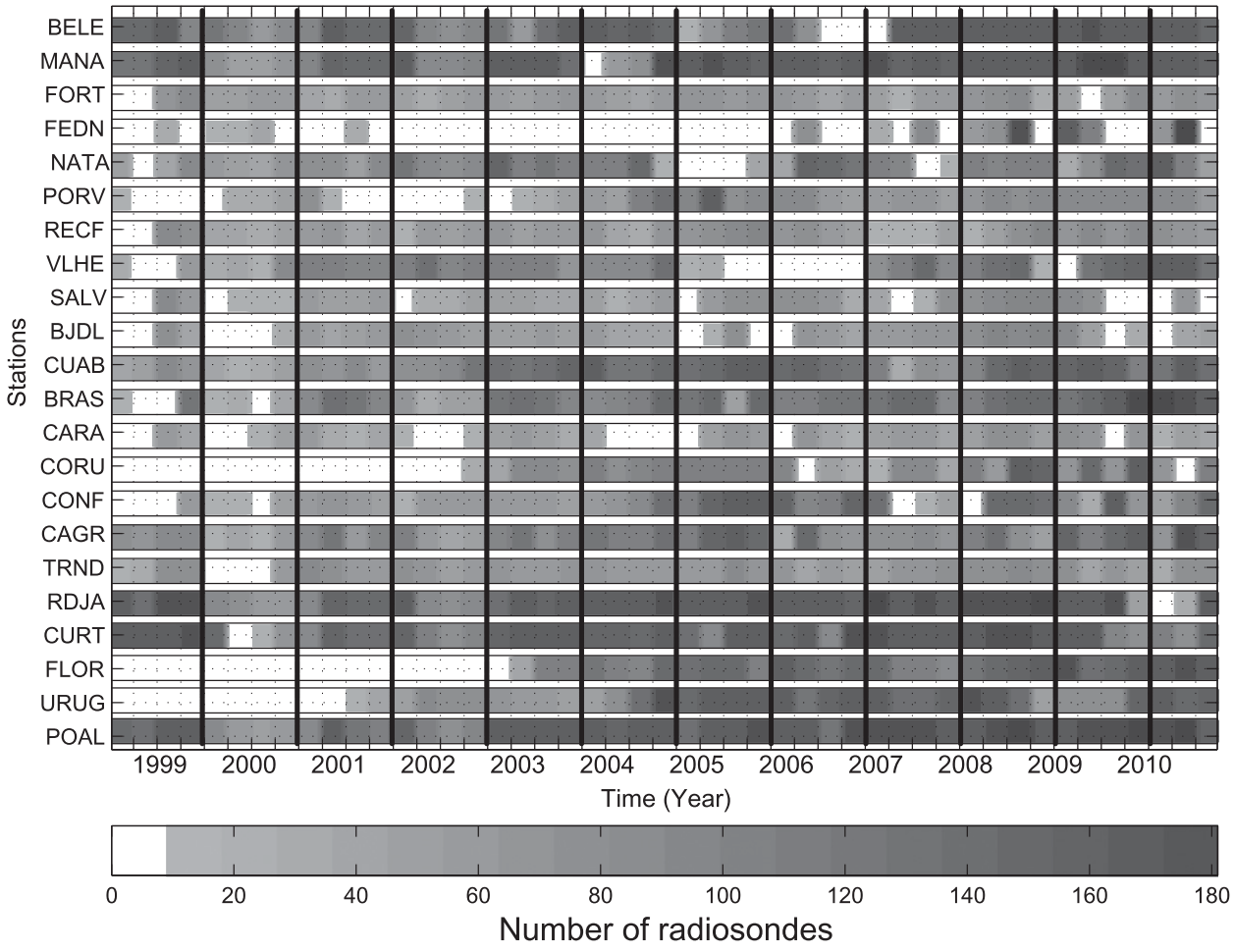

FIG. 2. Temporal distribution of the radiosonde dataset used in the evaluation of Tm modeling in a trimester.

how much of the differences between the models and the radiosonde is due to variability in the amount of water vapor. The results show that the uncertainty of the Tm values is larger when the water vapor concentration is lower, which is a result that confirms that for middle to higher latitudes, where the temperature is lower and the water vapor concentration is smaller, the Tm models are less skillful. On the other hand, in this region, the skill of the Tm models is less important because the zenith wet delay (Z_{WD}) values (see appendix A) are lower than in the tropical regions and, consequently, the propagation of the uncertainty in the Tm in the IWV values is also lower.

A seasonal analysis of the RMSE values from the four best models (MENDE, REGIO, BRAZI, and SCHU3) at each radiosonde station using the complete dataset (78 095 radiosondes) is shown in Fig. 7, in which the stations are arranged by latitude in ascending order. The results indicate a seasonal influence of the latitude on the performance of the models. For the stations at low latitudes, the RMS error of the models was 1–2 K; for the stations at higher latitude, the RMS error was 2–3 K in summer and 3–4 K in winter. These results are consistent with Fig. 6 because the Tm errors are smaller when the IWV is higher. The REGIO and BRAZI models presented very similar results. However, at the CUAB, CURU, TRND, and BJDL stations, the REGIO model presented worse results than the BRAZI model, which indicates that for these stations, the set of radiosondes used in the regional model is not entirely sufficient. The MENDE model tends to be better at low latitudes than at middle latitudes, especially during the summer. This model was the best at some stations, such as PORV, VLHE, TRND, and BJDL, during summer and spring, and at the BELE and MANA stations during summer and autumn. In contrast, the SCHU3 model had better results for the middle-latitude stations than for those at low latitude, again, independent of season. The regional models were better than the other models, independent of season, at most stations.

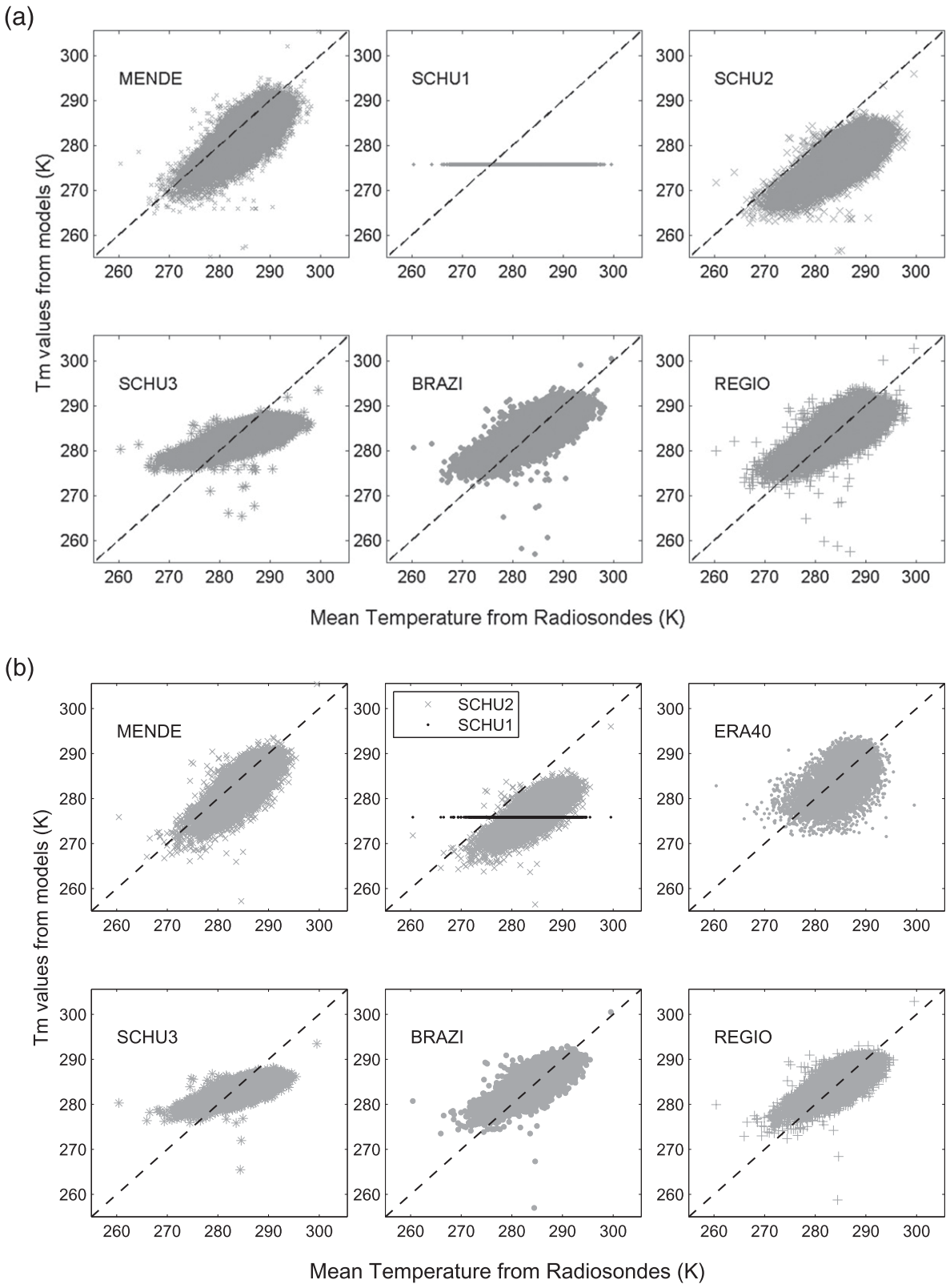

FIG. 3. Scatter diagrams of the Tm values from the model vs the mean values from the radiosondes used in the study: (a) complete period and (b) period from 1999 to 2002.

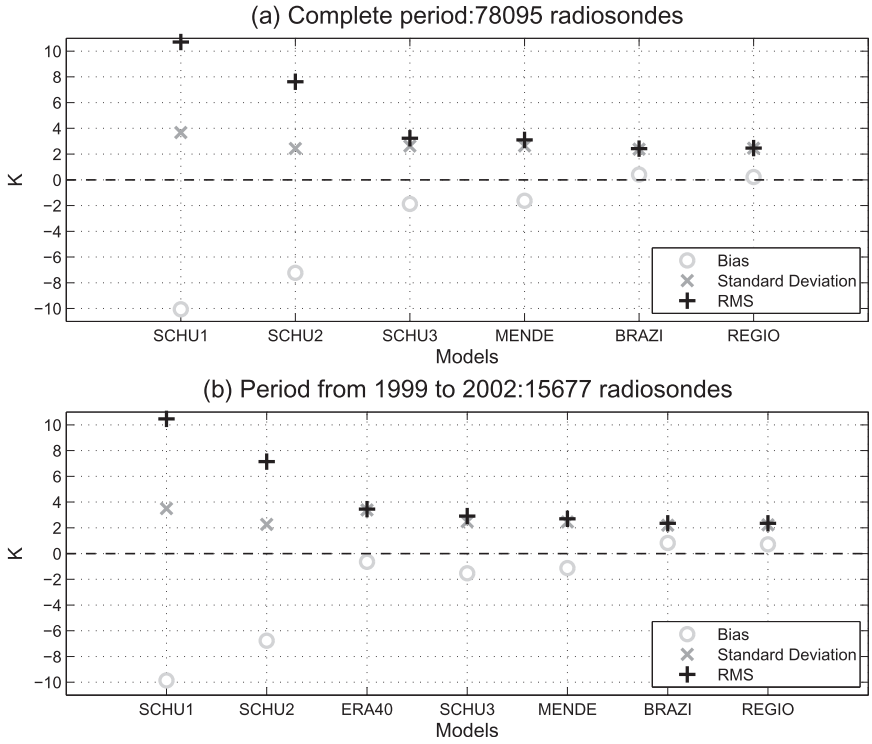

FIG. 4. The bias, SD, and RMSE values from the different Tm models evaluated using radiosonde values as a reference: (a) complete period and (b) period from 1999 to 2002.

b. *Performance evaluation of the* Tm *models in terms of the* IWV *estimates produced*

To evaluate the influence of the uncertainty of the Tm values on the final precision of the IWV estimates, the Z_{WD} values were calculated using radiosonde data by applying Eq. (A1) and converting the results to IWV using the Tm values from the different models. The same Z_{WD} values were converted to IWV using the Tm values obtained from the radiosonde data, which were used to evaluate the Tm models, and the bias, SD, and RMSE were then calculated. Figure 8 shows the IWV statistics using the dataset from 1999 to 2002, in which ERA-40 is also available, and Table 2 lists the values generated by using the complete dataset in a seasonal analysis. The results presented in Fig. 8 indicate that the influence of the Tm values on the IWV is greater than $0.3\,\mathrm{kg\,m^{-2}}$ (values presented by the SCHU3, MENDE, BRAZI, and REGIO models). The previous work that compared GPS and radiosonde results using data collected over the Amazon region reported a difference of approximately $3.7\,\mathrm{kg\,m^{-2}}$ (Sapucci et al. 2007). This result means that the influence of the Tm values reported above is nearly 10% of this difference. Figure 8 also shows that this influence can be as high as $1.4\,\mathrm{kg\,m^{-2}}$ if the SCHU1 model is used, in which a bias of $-1.3\,\mathrm{kg\,m^{-2}}$ was observed. ERA-40 presented almost no bias; however, the standard deviation and RMSE values were on the order of $0.45\,\mathrm{kg\,m^{-2}}$. The values presented in Table 2 also indicate that during the summer and spring the MENDE model presented no bias and had an RMSE of $0.26\,\mathrm{kg\,m^{-2}}$, and, consequently, it performed better than the other models. In contrast, during the autumn and winter, the BRAZI and REGIO models present lower biases, and in winter, these models had RMSE values of 0.23 and $0.24\,\mathrm{kg\,m^{-2}}$, respectively.

c. *Additional comments*

The REGIO model developed here for the southern region of Brazil has been used in the first experiment for the evaluation of IWV-GNSS in Argentina (Fernández et al. 2010). Three stations were used, with the results showing that the REGIO model gave an error in IWV directly proportional to the distance between these stations and the radiosondes used in the modeling. The RMSE values from the REGIO model at the stations closer to Brazil are smaller than the ones from the Tm model developed by Bevis et al. (1992). The Bevis model could be an option for use across Argentina because the radiosondes used in this modeling were launched at stations over the United States between 27° and 65°N,

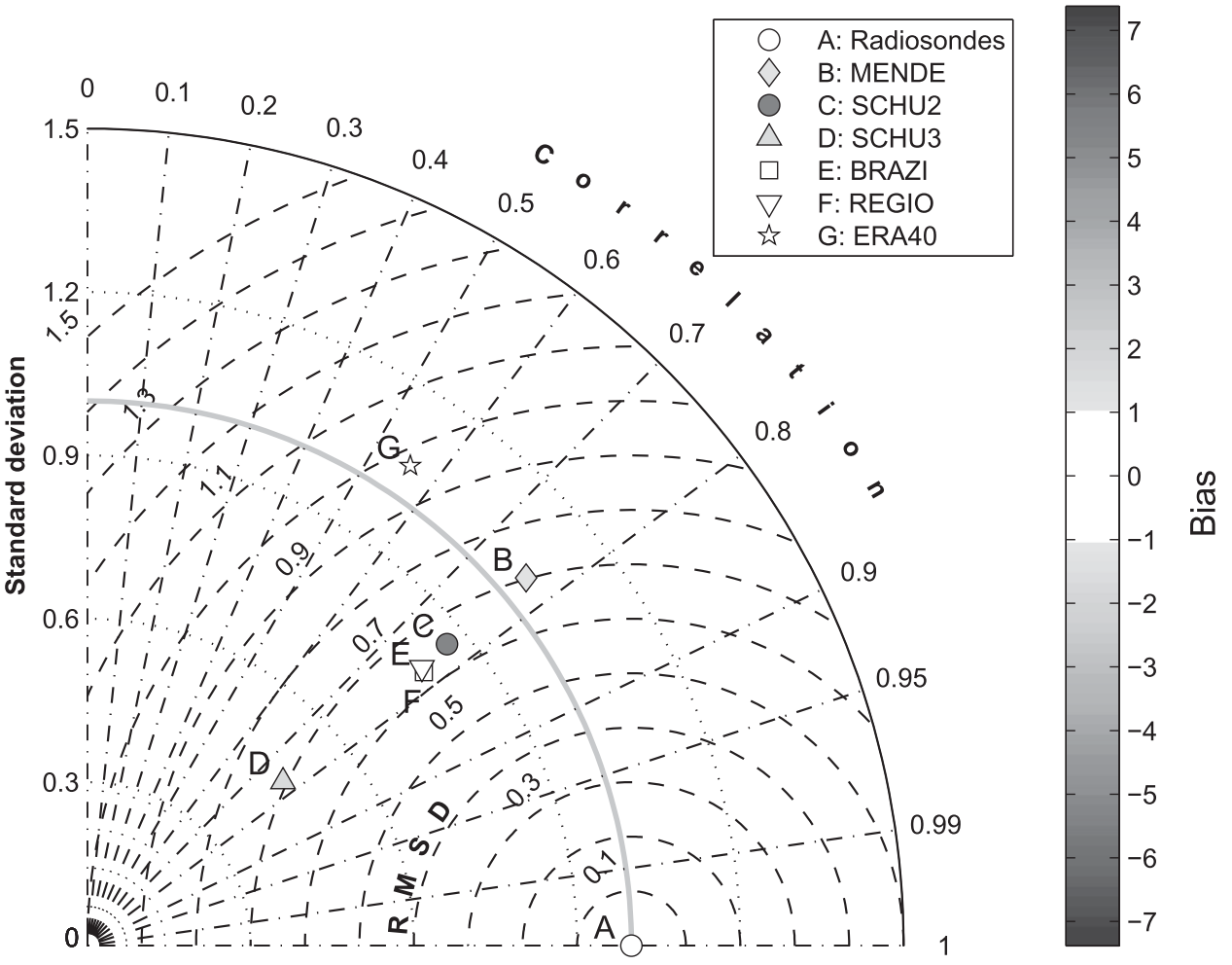

FIG. 5. Taylor diagram for the different Tm models and reanalysis using the dataset of radiosondes launched during the period from 1999 to 2002.

corresponding to the same latitude band as Argentina in the Southern Hemisphere.

Over the past 50 yr, studies of the accuracy and homogeneity of the world's upper-air observation system have been conducted in several international intercomparison experiments. The most recent experiments occurred in the United Kingdom (1984), the United States (1985), the former Soviet Union (1989), Japan (1993), the United States–Russian Federation (1995), Brazil (2001), Mauritius (2005), and China (2010) (Nash et al. 2011). Many important results were obtained from these experiments. Because the RS80 (Vaisala) radiosonde was very widely used in operational mode, it was the object of several studies aiming at evaluating the need for corrections due to the contamination of the electronic device of the humidity sensor (Wang et al. 2002). An altitude-independent scale factor in the lower troposphere has been used to reduce the RS80 (Vaisala) variability (Turner et al. 2003). A more sophisticated methodology for measuring atmospheric humidity based on a chilled-mirror hydrometer sensor was demonstrated by Fujiwara et al. 2003. This sensor was used to evaluate the accuracy and performance in tropical regions of the Vaisala RS80, RS90, and radiosondes from other manufacturers (Sapucci et al. 2005). A more recent intercomparison experiment evaluated the improvement developed by radiosonde manufacturers in the quantification of the atmospheric humidity (Sun et al. 2010). The problems identified in these intercomparison experiments contaminate the dataset used in the Tm modeling and, consequently, could be responsible for part of the uncertainty in the IWV obtained from the GNSS data.

4. Summary and conclusions

This study has presented an evaluation of the models available to determine the water-vapor-weighted mean

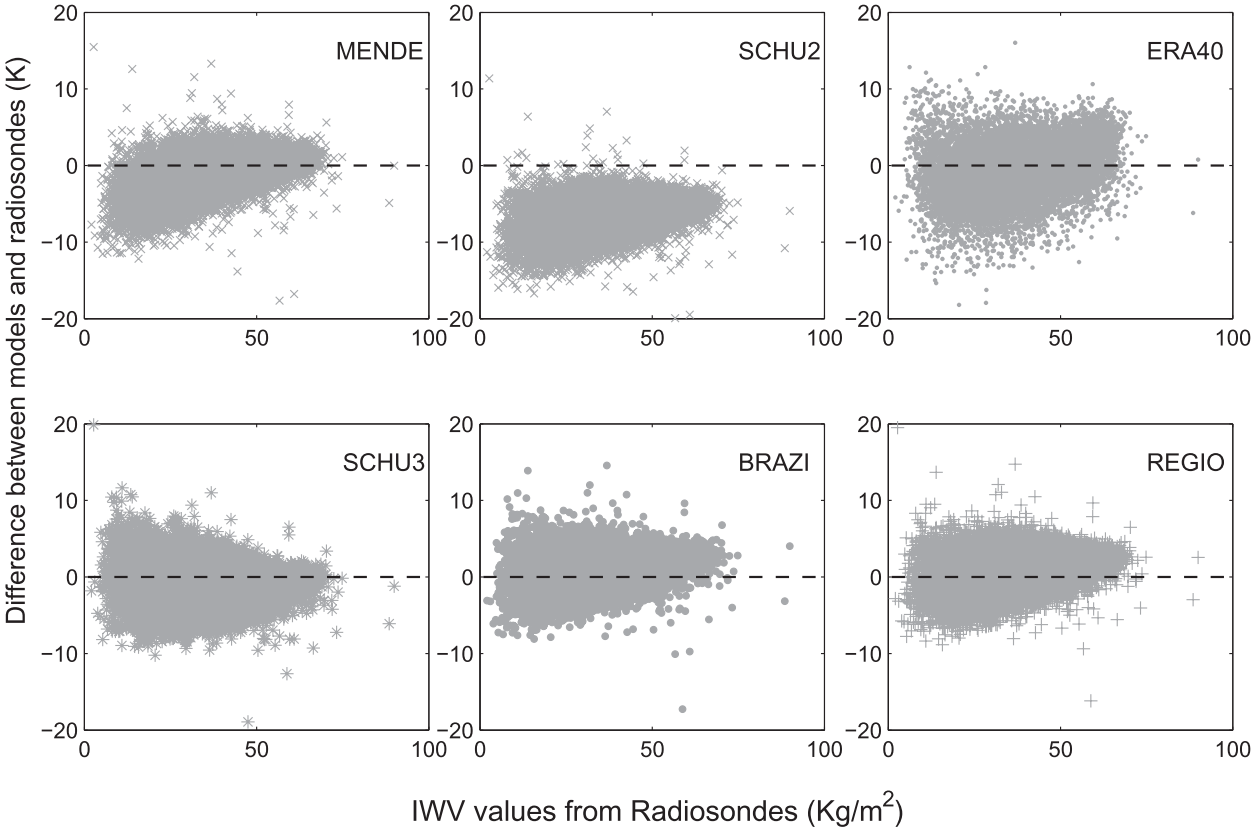

FIG. 6. Scatter diagram of the Tm error from the models vs the IWV values from radiosondes launched during the period from 1999 to 2002.

tropospheric temperature. The main objective of this study was to minimize the uncertainty in the determination of the IWV values from the ground-based GNSS network receivers over Brazil. A dataset of 78 000 radiosondes launched at 22 stations during the period of 1999–2010 was used. Five global and two regional models were evaluated. One global model is based on radiosondes, three are based on NWP products, and the last is based on reanalysis data. The regional models evaluated an applied multivariate statistical analysis over an independent radiosonde dataset of ~90 000 profiles collected at 12 Brazilian stations over a period of 32 yr (1961–93).

The results, taking into consideration all the stations, indicated that the RMS error values presented by the REGIO and BRAZI models are either similar to or lower than those of the other models (RMSE of 2.2 K); the models MENDE, SCHU3, and ERA-40 presented RMSEs of 2.8, 2.9, and 3.5 K, respectively, and the RMSEs for SCHU1 and SCHU2 were greater than 7.0 K. The ERA-40 presents almost no bias, but the dispersion is larger than that of the other model (SD of 3.5 K).

A seasonally dependent influence of the latitude on the performance of the models was observed, in which the RMS error of the Tm models is 2 K in stations at low latitudes and 2–4 K in stations of higher latitude. The REGIO and BRAZI models presented very similar results, and at most stations, they were better than the other models, independent of the season. There are stations at which the BRAZI model is better, and other stations at which the regional model performed poorly. The MENDE model tends to be better at low latitudes than at middle latitudes, and the SCHU3 model has the opposite behavior.

The impact of the Tm modeling on the IWV values was evaluated, and the results indicate that the influence of the uncertainty in the Tm values on the final precision of the IWV estimates is approximately 0.3 kg m^{-2}, which is the value presented by the SCHU3, MENDE, BRAZI, and REGIO models. The RMSE value from ERA-40 was 0.45 kg m^{-2}. In a seasonal evaluation taking into consideration all stations, the MENDE model was found to be the best model during summer and spring (RMSE of 0.26 kg m^{-2}), and the BRAZI and REGIO models presented the best results during autumn and winter (RMSEs of 0.23 and 0.24 kg m^{-2}, respectively). A possible reason for this seasonal dependence is that

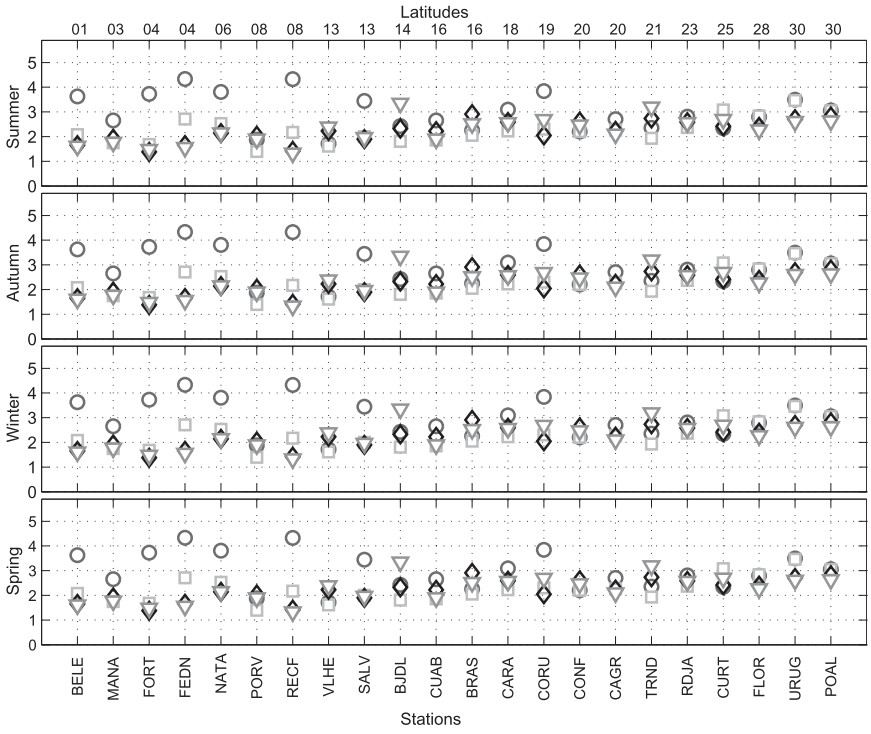

FIG. 7. Seasonal analysis of the RMSE of the Tm values from the four best models (squares, MENDE; triangles, REGIO; diamonds, BRAZI; and circles, SCHU3) for each radiosonde station using the complete dataset.

during winter and autumn, the penetrations of cold fronts from Antarctica have more influence on the Tm values over Brazil; consequently, the regional models are more appropriate than the global models. During summer and spring, the behavior of the atmosphere in this region is similar to the global mean, and in this case, the Mendes model (a global model) is better than the regional versions. The BRAZI and MENDE models can be used alternately to provide the best results for each station; thus, the results presented in Fig. 7 should be used to select the more appropriate model. The MENDE model should be used for 7 stations (PORV, VLHE, BJDL, BRAS, CARA, CONF, and TRND) and the BRAZI model should be used for the 15 other stations.

The evaluation of the Tm models indicated that those simulations based on radiosondes performed better than the ones based on the NWP results. The SCHU3 model and the ERA-40 values are affected by errors in the NWP profiles used in the Tm modeling. However, increased computational power, improved global observation systems, and advances in assimilation systems indicate that reanalyses may be more successful for Tm

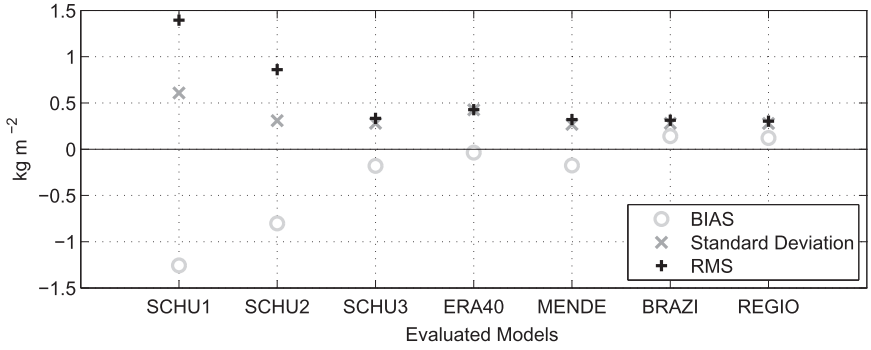

FIG. 8. Evaluation of the performance of the Tm models in the calculation of the IWV values using radiosondes as a reference.

TABLE 2. Bias, SD, and RMSE in the IWV values (kg m^{-2}) generated by the different models for each season.

	Summer			Autumn			Winter			Spring		
Model	Bias	SD	RMSE	Bias	SD	RMSE	Bias	SD	RMSE	Bias	SD	RMSE
SCHU1	−1.50	0.52	1.59	−1.34	0.61	1.47	−1.17	0.58	1.31	−1.37	0.56	1.48
SCHU2	−0.88	0.28	0.92	−0.88	0.30	0.93	−0.80	0.32	0.86	−0.81	0.30	0.87
SCHU3	−0.18	0.28	0.34	−0.25	0.25	0.36	−0.29	0.25	0.38	−0.20	0.30	0.36
BRAZI	0.21	0.28	0.35	**0.07**	**0.28**	**0.29**	**−0.02**	**0.23**	**0.23**	0.15	0.27	0.31
REGIO	0.17	0.30	0.34	0.04	0.29	0.30	−0.03	0.24	0.24	0.12	0.28	0.30
MENDE	**−0.01**	**0.25**	**0.26**	−0.16	0.26	0.30	−0.21	0.23	0.31	**−0.04**	**0.25**	**0.26**

modeling in the future. A new reanalysis, with better resolution and taking into consideration the large quantity of data now available, should be reevaluated. For this purpose, the ERA-Interim reanalysis is the best candidate. In addition, a regional reanalysis over South America, with 20-km horizontal resolution and covering a period of 12 yr (2000–11), is being developed by CPTEC. The performance of these reanalyses in the Tm modeling should be evaluated in future studies, in which other more appropriate methods for dividing the Brazilian region can be implemented. The climate regimes are good options because they can be used to distinguish suitably baroclinic atmospheres from tropical ones and, consequently, capture most of the variability in the water-vapor-weighted mean tropospheric temperature in this region.

Acknowledgments. The author thanks Luiz Augusto Toledo Machado and João Francisco Galera Monico for helpful comments and supervision in the development of the regional model, Derek Valério Schubert de Sousa for assistance in the data analysis, and the three anonymous reviewers for their significant help in improving the final version of the manuscript in its scientific content. Special thanks are given to the Departamento de Ciências Atmosféricas (ACA) do Instituto Aeronáutica e Espaço (IAE) do Centro Técnico Aeroespacial (CTA) de São José dos Campos-SP for the availability of the radiosonde temporal series, to Fundação de Amparo a Pesquisa do Estado de São Paulo (FAPESP), which indirectly supported this research [Grants Process 2006/04008-2 (GNSS-SP Project) and 2009/15235-8 (CHUVA project)], and to the Contractual Instrument of the Thematic Network of Geotectonic Studies CT-PETRO (PETROBRAS) and the INPE (Grant 600289299).

APPENDIX A

Mean Tropospheric Temperature in the IWV Measurements from GNSS Data

The mean influence of the electrically neutral atmospheric layer on GNSS signal propagation in the zenith direction, referred to as zenith tropospheric delay (Z_{TD}), is divided into two components: zenith wet delay (Z_{WD}), which is caused by atmospheric water vapor, and zenith hydrostatic delay (Z_{HD}), which is the total delay due to the other well-mixed gases and water vapor that compose the atmosphere (Spilker 1994). Assuming that hydrostatic equilibrium in the atmosphere is satisfied, the hydrostatic component (Z_{HD}) depends only on the total mass of the atmosphere, and, consequently, the values can be determined from pressure measurements at the surface (Davis et al. 1985). The Z_{WD} values are obtained by subtracting the Z_{HD} values from the total Z_{TD} estimated from GNSS observation processing. The Z_{WD} values can be extracted from the temperature and water vapor pressure profiles as follows (Spilker 1994):

$$Z_{WD} = 10^{-6} Z_w^{-1} \int \left(k_2' \frac{e}{T} + k_3 \frac{e}{T^2} \right) dh, \qquad \text{(A1)}$$

where e is the partial pressure of the water vapor, T is the air temperature, Z_w is the water vapor compressibility factor, and $k_2' = 22.10\,\text{K hPa}^{-1}$ and $k_3 = 373\,900\,\text{K}^2\,\text{hPa}^{-1}$ are the atmospheric refractivity constants (Bevis et al. 1994). Rearranging Eq. (A1) and applying the ideal gas law, while noting that IWV is the vertical integral of water vapor density, we can write

$$\begin{aligned} Z_{WD} \times 10^6 &= \left(k_2' + k_3 \frac{\int \frac{e}{T^2} dh}{\int \frac{e}{T} dh} \right) \int \frac{e}{T Z_w} dh \\ &= R_w \left(k_2' + k_3 \frac{\int \frac{e}{T^2} dh}{\int \frac{e}{T} dh} \right) \text{IWV}, \qquad \text{(A2)} \end{aligned}$$

where $R_w = 461.5181\,\text{J kg}^{-1}\,\text{K}^{-1}$ is the specific gas constant for water vapor. This equation presents a relationship between Z_{WD} and the IWV values, but it depends on the relationship between the humidity and temperature profiles. Consequently, the upper-air profile information is necessary, in addition to the surface measurements

from the GNSS receiver and surface meteorological stations. A method for solving this problem was presented by Davis et al. (1985), in which the mean value theorem for integration was applied. This theorem enables us to affirm that if $F:[a,b]\rightarrow\Re$ is a continuous function and G is an integrable function that does not change sign on the interval (a, b), then there is a number $y \in (a, b)$ such that

$$\int_b^a F(x)G(x)\partial x = F(y)\int_b^a G(x)\partial x. \qquad \text{(A3)}$$

Hence, assuming $F(h) = T$ and $G(h) = e/T^2$, for which the condition mentioned above is satisfied in the moisture-containing layer extending from the surface at height h_0 to the top of the troposphere h_{top}, there is a point $t \in (h_0, h_{\text{top}})$ where $F(t) = \text{Tm}$, which produces

$$\int_{h_0}^{h_{\text{top}}} T\frac{e}{T^2}\partial h = F(t)\int_{h_0}^{h_{\text{top}}}\frac{e}{T^2}\partial h \Rightarrow \int_{h_0}^{h_{\text{top}}}\frac{e}{T}\partial h$$

$$= \text{Tm}\int_{h_0}^{h_{\text{top}}}\frac{e}{T^2}\partial h \Rightarrow \text{Tm} = \frac{\displaystyle\int_{h_0}^{h_{\text{top}}}\frac{e}{T}\partial h}{\displaystyle\int_{h_0}^{h_{\text{top}}}\frac{e}{T^2}\partial h}. \qquad \text{(A4)}$$

As only values of temperature from the moist layer are taken into account in the determination of Tm [where $e \neq 0$ in the Eq. (A4)], this amount is denoted the water-vapor-weighted mean tropospheric temperature. Applying Eq. (A4) to Eq. (A2) gives

$$\text{IWV} = Z_{\text{WD}}\left[10^6\Big/R_w\left(k_2' + \frac{k_3}{\text{Tm}}\right)\right]. \qquad \text{(A5)}$$

The last equation is the relationship between the IWV and the zenith tropospheric delay, which is independent of any additional information other than the surface measurements (Bevis et al. 1992). Applying propagation variance theory (Ku 1966) to Eq. (A5) results in the following equation:

$$\sigma_{\text{iwv}}^2 = \left[\frac{10^6 \times Z_{\text{WD}}R_wK_3}{(R_wK_3 + R_wK_2'T_m)^2}\right]^2\sigma_{\text{Tm}}^2, \qquad \text{(A6)}$$

where σ_{iwv} and σ_{Tm} are the standard deviations of the IWV and Tm, respectively. This equation permits the assessment of the influence of the uncertainty in Tm on the IWV-GNSS estimates.

APPENDIX B

Tm Modeling over Brazil Using Multivariate Statistical Analysis

a. Dataset availability and data processing

The radiosonde dataset used in this modeling simulation, which was obtained from instruments launched by the Detachment of Airspace Protection and operated by the Brazilian Air Force, is composed of 91 136 radiosondes launched at 12 Brazilian airports during the period from 1961 to 1993. This dataset and the one presented in section 3, which is used in the evaluation of the model, are independent. An analysis of the consistency of temperature, pressure, and humidity profiles was performed using a quality control process, in which the problematic profiles were removed. A total of 1522 profiles (~1.7% of the complete dataset) were excluded, and the final dataset was composed of 89 614 radiosondes. The list of stations used for the radiosondes launched for this dataset is given in Table 1, which presents the station ID numbers and coordinates, as well as the numbers of radiosondes launched at each site. The spatial distribution of these stations is shown in Fig. 1. The total dataset was divided into five groups, one for each Brazilian climatic region. The criterion for the climate zones was the location of the radiosondes. The radiosondes launched at the Porto Alegre and Curitiba stations were grouped to compose the southern region, which has a climate highly influenced by cold fronts from the middle latitudes. The radiosondes launched in the states of São Paulo and Rio de Janeiro were grouped to form the subtropical oceanic region, and the radiosondes launched at Brasilia and Campo Grande form the subtropical continental region. The radiosondes launched at Natal and Fernando de Noronha were denoted the northeastern region group, and the radiosondes launched at the Manaus, Alta Floresta, Belém, and Vilhena stations comprised the northern region.

Values of Tm were calculated using the data from the radiosonde temperature and humidity profiles to numerically integrate Eq. (1). The measurements of temperature (Ts), relative humidity (RH), pressure (Ps), and wind direction and wind speed from the first level of the radiosonde vertical profile were considered to be those measured at the surface. The wind direction and wind speed were converted into their zonal (U) and meridional components (V). Several radiosondes experienced technical problems and were not able to measure wind information. A second radiosonde set with 71 994 profiles was organized, in which the radiosondes without wind information were excluded to avoid erroneous

TABLE B1. Weights of the variables (columns 2–5) for each factor obtained in the factor analysis and their communality; and the variance and the percentage of the total variance explained by each factor and the communality. The key values are shown in boldface.

Variables	Factor 1	Factor 2	Factor 3	Factor 4	Communality
Ps	**0.664**	−0.376	−0.292	0.129	0.684
Ts	**0.888**	0.240	0.014	−0.047	0.849
RH	−0.149	**−0.937**	−0.002	0.032	0.902
U	−0.057	−0.039	0.055	**0.989**	0.987
V	0.024	−0.011	**−0.980**	−0.060	0.964
Tm	**0.908**	0.130	0.050	−0.116	0.858
Variance	2.082	1.096	1.051	1.016	5.2446
Variance explained (%)	**34.7**	**18.3**	**17.5**	**16.9**	**87.4**

conclusions in the analysis generated by a different population of the variables evaluated.

b. *Factor analysis of the data variance*

In factor analysis, the variables related to a dataset can be grouped by applying criteria of similar correlations to each group, denoted factors (Johnson and Wichern 1992). This method describes, where possible, the relationship among the set of variables in terms of a potentially lower number of unobserved variables (factors), reducing the data in the analysis with a minimum loss of information and facilitating the interpretation of results obtained (exploratory factor analysis). The factor analysis estimates how much of the variance is due to common factors, which is very useful information that is called communality (Johnson and Wichern 1992).

The first step in the factor analysis is the selection of the most appropriate variables to reach the intended objectives because the inclusion of inappropriate variables can generate flotation in the final variance of the dataset, which prejudices the interpretation of the results. Taking into consideration that the objective of this analysis is to define which variables measured at the surface are most relevant to modeling Tm, the variables related to position (latitude and longitude) and time (day, month, etc.) and those obtained indirectly by calculation (IWV, moist layer height, and arithmetical mean of the temperature profile) are not included in this analysis. The selected variables were pressure (Ps), temperature (Ts), relative humidity (RH), and the zonal (*U*) and meridional (*V*) wind components. The factoring was performed by principal component analysis (PCA) using the correlation matrix of the variables selected. A varimax rotation was applied to the factors to make them more understandable and to facilitate their interpretation. Table B1 lists the weights of each variable in the four factors generated, as well as the respective communality, variance, and percentage of the total variance explained by each one.

The first four factors explain 87.4% of the total variance of the dataset, and this result indicates that the number of factors used can be considered suitable for this analysis. The weights of the factors presented in Table B1 indicate that the evaluated variables can be divided into four correlation groups. The first group, defined as factor 1, is formed by temperature, surface pressure, and mean tropospheric temperature, which explain 34.7% of the total variance of the dataset. The relative humidity, the meridional component of the wind, and the zonal component of the wind comprise, individually, the three other groups, which are indicated by factors 2, 3, and 4, respectively. The key values are shown in boldface in Table B1. The grouping generated by this factor analysis reveals that, in addition to surface temperature, the pressure values can be useful in the modeling of Tm. In contrast, the results indicate that

TABLE B2. As in Table B1, but for the first two factors obtained in the factor analysis in each of the five climate regions. The key values are shown in boldface.

	South		Subtropical ocean		Subtropical continent		Northeast		North	
Variance	Factor 1	Factor 2	Factor 1	Factor 2	Factor 1	Factor 2	Factor 1	Factor 2	Factor 1	Factor 2
Ps	0.1	**0.9**	**0.8**	−0.3	0.1	0.0	0.0	−0.0	**0.9**	0.2
Ts	**0.9**	0.1	**0.8**	0.4	**0.9**	−0.2	**−0.8**	0.3	**0.9**	−0.3
RH	**−0.6**	−0.4	−0.1	**−0.9**	**−0.6**	−0.6	**0.8**	−0.4	−0.2	**0.9**
U	−0.1	−0.0	0.0	0.0	0.1	**−0.9**	0.2	**−0.9**	−0.2	0.1
V	−0.1	0.0	−0.1	−0.1	−0.1	0.0	0.0	−0.1	0.0	−0.0
Tm	**0.9**	0.0	**0.9**	0.3	**0.8**	0.1	**−0.9**	−0.0	**0.8**	−0.3
Variance	1.8	1.1	1.8	1.1	1.8	1.2	2.0	1.2	2.1	1.1
% variance	**29.6**	18.5	**29.6**	18.5	**30.3**	20.4	**33.6**	19.5	**35.5**	19.0

TABLE B3. Values of the coefficients of the linear regression given by Eq. (A8) specific to each climatic region.

Climate region	No. of radiosondes	Coefficients of Eq. (A8)				R^2
		a	b	c	d	
South	24 065	0.613 90	0	0.020 243	102.815	0.590
Subtropical ocean	23 964	0.558 43	0.012 719	0	108.149	0.602
Subtropical continent	16 091	0.443 30	0	−0.032 011	155.717	0.424
Northeast	8158	0.362 78	0	−0.050 706	183.950	0.297
North	17 336	0.522 86	0.004 765	0	126.612	0.356

values from other surface variable do not significantly contribute to improvements in modeling Tm.

To assess the regional variations in the importance of the variables in the modeling of Tm, a similar factor analysis was performed for the climatic regions mentioned in the previous subsection, among which the radiosonde stations were divided. Table B2 presents the values of the weights for the first two factors and the respective variance and percentage of the total variance explained by each one.

The values in Table B2 indicate that the contribution of the humidity measurement at the surface to the Tm modeling depends on the region. This dependence is observed in the south, subtropical continental, and northeast regions. In the south and subtropical continental regions, the humidity values are related to the passage of cold fronts, which are very strong and frequent and cause large changes in the temperature profile. In the northeast region, these cold front events occur during some periods of the year; consequently, the relative humidity should contain a signal of the change in air mass. In the Amazon and ocean subtropical regions, this influence is rare, and the pressure at the surface is the main variable that is useful in Tm modeling. These results are used in the determination of suitable Tm models for each Brazilian region.

c. Tm *modeling for Brazil using multiple regressions*

Taking into consideration all the data, the response variables selected in the Tm model were based on the results of the factor analysis presented in Table B1. The weights of Ps and Ts in the first factor indicate that these are the predictors that explain the most variance in Tm. A statistical method that minimizes the residual least squares was applied to determine the values of the parameters. The Tm values from the regression generated in this process are given by the following equation:

$$\mathrm{Tm} = 0.558\mathrm{Ts} + 0.0105\mathrm{Ps} + 110.578, \qquad \text{(A7)}$$

which is denoted the Brazilian model here because it was obtained using the entire radiosonde dataset, and consequently, it can be applied throughout Brazil. The use of pressure measurements in the Tm model is expected because the greater the pressure at the surface, the deeper the atmospheric layer contributing to the warmer part of the sounding and, consequently, the larger the Tm values. The values of the coefficient of determination (R^2) indicate the percentage of the total variance of the response variable that is explained by the prediction variables used. The R^2 values closer to 1 indicate that the obtained model is efficient and that the residuals generated are closer to 0. The R^2 value obtained by this regression was 0.66.

The same technique applied to the radiosonde datasets selected for the climatic regions produced by the regional models. The prediction variables used in this case are also chosen by taking into consideration the results generated from the factor analysis (Table B2). The general equation for this model is

$$\mathrm{Tm} = a\mathrm{Ts} + b\mathrm{Ps} + c\mathrm{RH} + d, \qquad \text{(A8)}$$

where the values of the coefficients a, b, c, and d for each climatic region are presented in Table B3 and where the respective coefficient of determination values are also listed. These values show that the south and subtropical continental climatic region models exhibit similar percentages of total variance of Tm that are larger than those for the other regions. The R^2 values generated in the south and subtropical continental climatic regions were 0.59 and 0.60, respectively. The northeast region model had a lower coefficient of determination (0.30), perhaps due to the lower number of radiosondes available in this region.

REFERENCES

Adams, D. K., and Coauthors, 2011: A dense GNSS meteorological network for observing deep convection in the Amazon. *Atmos. Sci. Lett.,* **12,** 207–212.

Askne, J., and H. Nordius, 1987: Estimation of tropospheric delay for microwaves from surface weather data. *Radio Sci.,* **22,** 379–386.

Bevis, M., S. Susinger, T. Herring, C. Rocken, R. A. Anthes, and R. Ware, 1992: GPS meteorology: Remote sensing of atmospheric water vapor using the Global Positioning System. *J. Geophys. Res.,* **97** (D14), 15 787–15 801.

——, G. Chiswell, T. A. Herring, R. Anthes, C. Rocken, and E. R. H. Ware, 1994: GPS meteorology: Mapping zenith wet delays into precipitable water. *J. Appl. Meteor.,* **33,** 379–386.

Davis, J. L., T. A. Herring, I. Shapiro, A. E. Rogers, and G. Elgened, 1985: Geodesy by interferometry: Effects of atmospheric modeling errors on estimates of base line length. *Radio Sci.,* **20,** 1593–1607.

Deblonde, G., S. Macpherson, Y. Mireault, and P. Héroux, 2005: Evaluation of GPS precipitable water over Canada and the IGS network. *J. Appl. Meteor.,* **44,** 153–166.

Dick, G., G. Gendt, and C. Reigber, 2001: First experience with near real-time water vapor estimation in a German GPS network. *J. Atmos. Sol. Terr. Phys.,* **63,** 1295–1304.

Emardson, T. R., 1998: Studies of atmospheric water vapor using the Global Positioning System. School of Electrical and Computer Engineering Tech. Rep. 339, Charmers University of Technology, Göteborg, Sweden, 29 pp.

——, and H. J. P. Derks, 2000: On the relation between the wet delay and the integrated precipitable water vapour in the European atmosphere. *Meteor. Appl.,* **7,** 61–68, doi:10.1017/S1350482700001377.

Fernández, L. I., P. Salio, M. P. Natali, and A. M. Meza, 2010: Estimation of precipitable water vapour from GPS measurements in Argentina: Validation and qualitative analysis of results. *Adv. Space Res.,* **46,** 879–894.

Fujiwara, M., M. Shiotani, F. Hasebe, H. Vömel, S. J. Oltmans, P. W. Ruppert, T. Horinouchi, and T. Tsuda, 2003: Performance of the Meteolabor ''Snow White'' chilled-mirror hygrometer in the tropical troposphere: Comparisons with the Vaisala RS80 A/H-Humicap sensors. *J. Atmos. Oceanic Technol.,* **20,** 1534–1542.

Gregorius, T., 1996: How it works... GIPSY OASIS II. Dept. of Geomatics, University of Newcastle upon Tyne, 167 pp. [Available online at http://www.gps.caltech.edu/classes/ge167/file/gipsy-oasisIIHowItWorks.pdf.]

Guerova, G., E. Brockmann, J. Quiby, F. Schubiger, and C. Matzler, 2003: Validation of NWP mesoscale models with Swiss GPS Network AGNES. *J. Appl. Meteor.,* **42,** 141–150.

Herring, T. A., R. W. King, and S. C. Mcclusky, cited 2012: Documentations for the GAMIT–GLOBK GPS analysis software. Dept. of Earth, Atmospheric, and Planetary Sciences, Massachusetts Institute of Technology. [Available online at http://www-gpsg.mit.edu/~simon/gtgk/.]

Ingold, T., B. Schmid, C. Mätzler, P. Demoulin, and N. Kämpfer, 2000: Modeled and empirical approaches for retrieving columnar water vapor from solar transmittance measurements in the 0.72, 0.82, and 0.94 absorption bands. *J. Geophys. Res.,* **105,** 24 327–24 343.

Jade, S., M. S. M. Vijayan, V. K. Gaur, Tushar, P. Prabhu, S. C. Sahu, 2005: Estimates of precipitable water vapour from GPS data over the Indian subcontinent. *J. Atmos. Sol. Terr. Phys.,* **67,** 623–635.

Johnson, R. A., and D. W. Wichern, 1992: *Applied Multivariate Statistical Analysis*. Pearson, 800 pp.

Ku, H. H., 1966: Notes on the use of propagation of error formulas. *J. Res. Natl. Bur. Stand.,* **70C,** 262.

Liou, Y.-A., Y.-T. Teng, T. Van Hove, and J. C. Liljegren, 2001: Comparison of precipitable water observations in the near tropics by GPS, microwave radiometer, and radiosondes. *J. Appl. Meteor.,* **40,** 5–15.

Mendes, V. B., G. Prates, L. Santos, and R. B. Langley, 2000: An evaluation of the accuracy of models for the determination of the weighted mean temperature of the atmosphere. Preprints, *13th IONGPS Int. Tech. Meeting,* Anaheim, CA, Institute of Navigation. [Available online at gauss.gge.unb.ca/papers.pdf/ion2000ntm.pdf.]

Monico, J. F. G., P. de Oliveira Camargo, D. B. Marra Alves, and G. P. dos S. Rosa, 2009: São Paulo state continuous GNSS network: status and services available. *Proc. Geodesy for Planet Earth,* Buenos Aires, Argentina, Int. Association of Geodesy.

Nash, J., T. Oakley, H. Vömel, and LI Wei, 2011: WMO intercomparison of high quality radiosonde systems. WMO Rep. 107, WMO/TD-No. 1580, 248 pp.

Rocken, C., T. Van Hove, and R. H. Ware, 1997: Near real-time GPS sensing of atmospheric water vapor. *Geophys. Res. Lett.,* **24,** 3221–3224.

Ross, R. J., and S. Rosenfeld, 1997: Estimating mean weighted temperature of the atmosphere for Global Positioning System applications. *J. Geophys. Res.,* **102** (D18), 21 719–21 730.

Sapucci, L. F., L. A. T. Machado, R. B. Silveira, G. Fisch, and J. F. G. Monico, 2005: Analysis of relative humidity sensors at WMO radiosonde intercomparison experiment in Brazil. *J. Atmos. Oceanic Technol.,* **22,** 664–678.

——, ——, and J. F. G. A. Plana-Fattori, 2007: Intercomparison of integrated water vapor estimates from multisensor in the Amazonian region. *J. Atmos. Oceanic Technol.,* **24,** 1880–1894.

Schueler, T., G. W. Hein, and R. Biberger, 2001: A global analysis of the mean atmospheric temperature for GPS water vapor estimation. Preprints, *14th IONGNSS Int. Tech. Meeting,* Salt Lake City, UT, Institute of Navigation.

Spilker, J., Jr., 1994: Tropospheric effects on GPS. *Global Positioning System: Theory and Applications,* B. L. Parkinson and J. J. Spilker Jr., Eds., Vol. 1, American Institute of Aeronautics and Astronautics, 517–546.

Sun, B., A. Reale, D. J. Seidel, and D. C. Hunt, 2010: Comparing radiosonde and COSMIC atmospheric profile data to quantify differences among radiosonde types and the effects of imperfect collocation on comparison statistics. *J. Geophys. Res.,* **115,** D23104, doi:10.1029/2010JD014457.

Taylor, K. E., 2001: Summarizing multiple aspects of model performance in a single diagram. *J. Geophys. Res.,* **106,** 7183–7192.

Turner, D. D., B. M. Lesht, S. A. Clough, J. C. Liljegren, H. E. Revercomb, and D. C. Tobin, 2003: Dry bias and variability in Vaisala RS80-H radiosondes: The ARM experience. *J. Atmos. Oceanic Technol.,* **20,** 117–132.

Van Baelen, J., J. P. Albagnag, and A. Dabas, 2005: Comparison of near–real time estimates of integrated water vapor derived with GPS, radiosondes, and microwave radiometer. *J. Atmos. Oceanic Technol.,* **22,** 201–210.

Vey, S., R. Dietrich, A. Rülke, M. Fritsche, P. Steigenberger, and M. Rothacher, 2010: Validation of precipitable water vapor within the NCEP/DOE Reanalysis using global GPS observations from one decade. *J. Climate,* **23,** 1675–1695.

Wang, J., H. L. Cole, D. J. Carlson, E. R. Miller, K. Beierle, A. Paukkunen, and T. K. Laine, 2002: Corrections of humidity measurements errors from the Vaisala RS80 radiosonde—Application to TOGA CARE data. *J. Atmos. Oceanic Technol.,* **19,** 981–1002.

——, L. Zhang, and A. Dai, 2005: Global estimates of water-vapor-weighted mean temperature of the atmosphere for GPS applications. *J. Geophys. Res.,* **110,** D21101, doi:10.1029/2005JD006215.